Ferro-orbital order in the charge- and cation-ordered manganite $YBaMn_2O_6$

Anthony J Williams and J Paul Attfield
Centre for Science at Extreme Conditions and School of Chemistry, University of Edinburgh, King's Buildings, Mayfield Road, Edinburgh, EH9 3JZ, United Kingdom
(Received 27 January 2005; published 18 July 2005)

Powder neutron diffraction reveals a subtle triclinic distortion in the 300 K structure of the Y^{3+}/Ba^{2+} cation-ordered and Mn^{3+}/Mn^{4+} charge-ordered perovskite $YBaMn_2O_6(Y_{0.5}Ba_{0.5}MnO_3)$. The refined structure shows a ferro-orbital ordering (FOO) in which d_z^2-type orbitals associated with the Jahn-Teller Mn^{3+} states are oriented in a parallel fashion. This ground state has not previously been found in $AMnO_3$ manganites, although the alternative antiferro-orbital ordering (AFOO) is commonly observed, for example, in the analog $TbBaMn_2O_6$. Lattice distortions that determine the balance between FOO and AFOO states result from the size mismatch between Y or Tb and Ba, and a high-temperature AFOO to FOO transition is evidenced in $TbBaMn_2O_6$.

DOI: 10.1103/PhysRevB.72.024436 PACS number(s): 71.45.Lr, 61.66.Fn, 75.47.Lx, 61.12.Ld

I. INTRODUCTION

Manganese oxide perovskites have been the focus of much research over the last decade to understand their physical properties such as colossal magnetoresistance.[1] The "cubic" $AMnO_3$ family ($A=L_{1-x}M_x$; L=trivalent lanthanide, M=Ca, Sr, Ba) exhibit a very rich phase diagram, with several ground states—principally the itinerant ferromagnetic and insulating charge-ordered antiferromagnetic states. The charge-ordered (CO) ground state is most readily observed in 50% doped ($x=0.5$) manganites. The first model for the CO phase (in $La_{0.5}Ca_{0.5}MnO_3$) was proposed by Goodenough[2] after the magnetic structure was determined to be of the complex CE type, with ferromagnetic couplings along zigzag chains.[3] "Checkerboard" layers of localized Mn^{3+} and Mn^{4+} states are stacked in a ferro- manner (directly above each other) to yield a "striped" CO arrangement. The structures of $La_{0.5}Ca_{0.5}MnO_3$ (Refs. 4 and 5) and several other half-doped manganites[6–9] have subsequently been shown to adopt this arrangement. An alternative CO ground state, in which the same checkerboard layers of Mn^{3+}/Mn^{4+} stack in an antiferro- (out of phase) sequence to give a "rocksalt" three-dimensional charge ordering, has recently been observed in the A-cation-ordered manganite $TbBaMn_2O_6$ at 300 K.[10]

In addition to the charge ordering, symmetry-breaking orbital ordering is also observed in many insulating manganites, as a result of cooperative Jahn-Teller distortions of the high-spin $3d^4Mn^{3+}$ configuration. The coupling of the localized d_z^2-type Mn^{3+} electron states to the lattice results in elongations of the corresponding Mn-O bonds that may be measured crystallographically. A theoretical model for manganites[11] has proposed that both antiferro-orbital-ordered [AFOO, an antiferroelastic phase; see Fig. 1(a)] and ferro-orbital-ordered [FOO, a ferroelastic; Fig. 1(b)] ground states are possible. AFOO accompanies both striped CO in $La_{0.5}Ca_{0.5}MnO_3$ and rocksalt CO in $TbBaMn_2O_6$, and is also found in undoped $LaMnO_3$, but the FOO state has not previously been reported in $AMnO_3$ manganites. Here we show that rocksalt charge ordering is accompanied by a ferro-orbital ordering in the 300 K structure of $YBaMn_2O_6$. A high-temperature AFOO to FOO transition is also evidenced in $TbBaMn_2O_6$. Magnetic and transport properties, and variable temperature structural studies of $YBaMn_2O_6$ have been reported previously.[12,13] A paramagnetic insulating phase was found between the Néel transition at 200 K and a charge-ordering transition at $T_{CO}=480$ K.

II. EXPERIMENT

An 8 g sample of polycrystalline $YBaMn_2O_6$ was prepared via the reduced intermediate $YBaMn_2O_5$.[14,15] This was prepared by sintering pellets of Y_2O_3, Mn_2O_3 and $BaCO_3$ under flowing argon at 1400 °C for 24 h, and was then oxidized to $YBaMn_2O_6$ by annealing in an O_2 flow at 300 °C for multiple periods of 12 h until there was no further gain in sample mass. The $YBaMn_2O_6$ sample was found to contain ~1% of a secondary phase, tentatively assigned as $BaMnO_{3-x}$. High-resolution time-of-flight powder neutron diffraction data were collected on the HRPD instrument at the ISIS spallation neutron facility, U.K. Profiles from the backscattering ($2\theta=168°$) and the $2\theta=90°$ detector banks were Rietveld analyzed simultaneously using the general structure analysis system (GSAS) program.[16]

III. STRUCTURE ANALYSIS AND DISCUSSION

The 300 K powder neutron diffraction pattern of $YBaMn_2O_6$ is similar to that of CO and AFOO $TbBaMn_2O_6$.[10] However, the ($h\,k/2\,l$) superstructure peaks that signify the AFOO in $TbBaMn_2O_6$ are absent in the profile of $YBaMn_2O_6$ at 300 K (Fig. 2), and at temperatures down to 4 K. CO distortions in these A-cation-ordered manganites lower the space group symmetry from tetragonal $P4/mmm$ for the aristotype $LaBaMn_2O_6$-type structure to monoclinic $P2_1/m$. This model gives a fairly good fit to the 300 K data (goodness of fit $\chi^2=15.54$, weighted residual $R_{wp}=7.87\%$ for eight symmetry-independent atoms, 18 refined variable coordinates) with refined lattice parameters $a=5.519\,07(1)$, $b=5.5133(1)$, $c=7.6020(1)$Å and $\beta=90.267(1)°$. The structure contains two distinct Mn sites

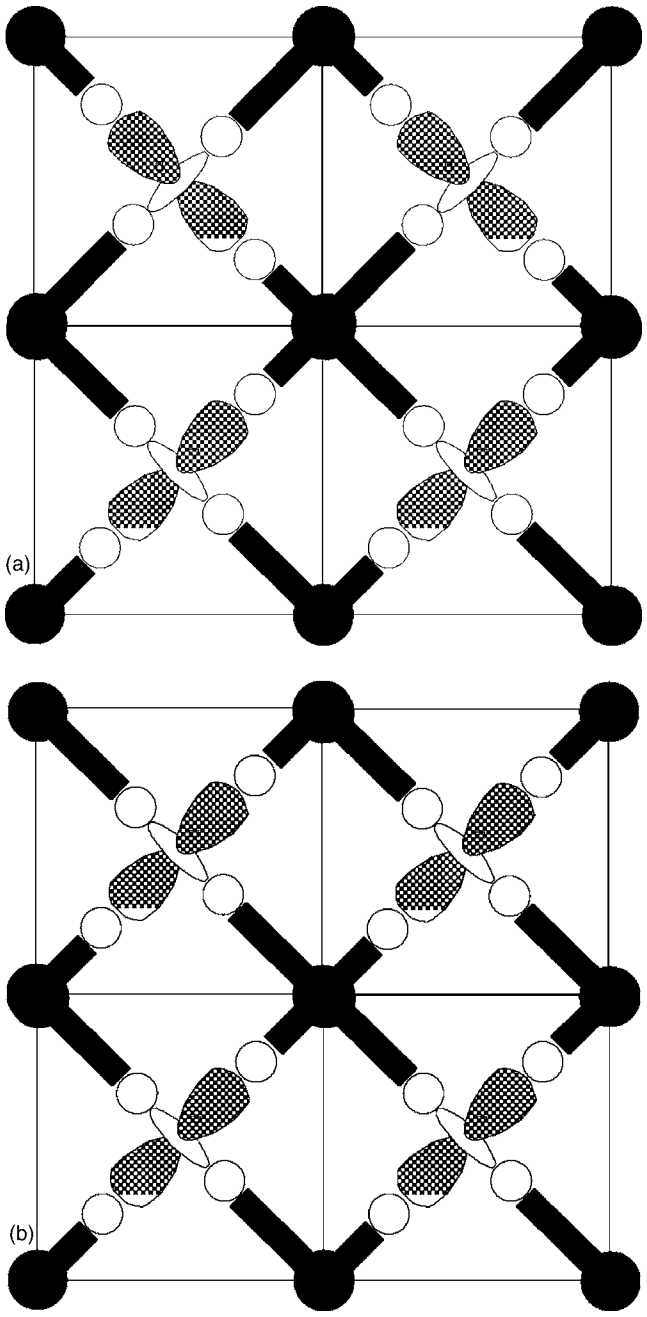

FIG. 1. The two idealized orbital orderings for the checkerboard charge-ordered layers of 50% doped manganites [Mn^{3+} shown as d_z^2-type orbitals; Mn^{4+} (oxygen) as filled (open) circles]: (a) antiferro-orbital order (AFOO); (b) ferro-orbital order (FOO). The consequent distortions around Mn^{4+} are shown.

corresponding to the rocksalt CO arrangement of Mn^{3+}- and Mn^{4+}-like states observed in $TbBaMn_2O_6$. Close inspection of the fit of the $P2_1/m$ model to the neutron data revealed additional broadenings of some reflections, for example (220) (Fig. 3). These partly resolved splittings evidence a further, subtle lowering of symmetry, from monoclinic to triclinic. This was confirmed by comparing Le Bail fits, in which no structural model is assumed, to the entire profile; χ^2 fell significantly from 14.61 for the $P2_1/m$ symmetry fit to 11.72 for triclinic $P\bar{1}$ symmetry.

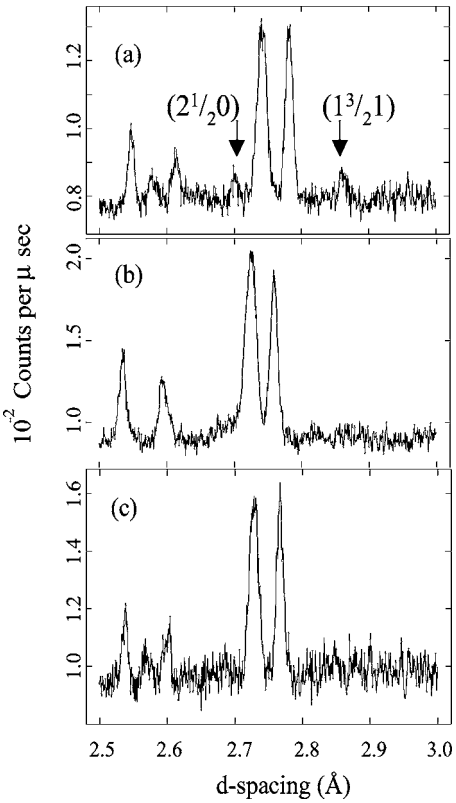

FIG. 2. Part of the 90° bank HRPD neutron powder diffraction profiles; the labeled reflections that evidence the $(0\frac{1}{2}0)$ AFOO superstructure of $TbBaMn_2O_6$ at 300 K in (a) are absent for $YBaMn_2O_6$ at 300 K (b), and for $TbBaMn_2O_6$ at 373 K (c).

Refinement of the $YBaMn_2O_6$ structure in space group $P\bar{1}$ gave the atom positions in Table I with cell parameters a =5.519 74(8), b=5.513 79(8), c=7.603 19(10)Å, and α =90.017(2)°, β=90.280(1)°, and γ=90.106(1)°.[17] The relatively large departure of γ from 90° accounts for the prominent broadening of (*hk0*) peaks such as (220) in Fig. 3. Refinement of the Y/Ba fractional occupancies showed no antisite disorder to within 2%, and no oxygen deficiency was evidenced. The derived Mn-O distances (Table II) show that the MnO_6 octahedra in the structure of $YBaMn_2O_6$ (Fig. 4) are highly distorted, in part by the strains that result from the size difference between the *A* cations (the mean Ba-O and Y-O distances are 2.84 and 2.65 Å, respectively). The difference between the mean Mn-O distances within the two octahedra confirms that CO is present. The bond valence sums (BVS)[18] for the Mn1 and Mn2 sites are, respectively, 3.36 and 3.81. We thus refer to the sites as being Mn^{3+} and Mn^{4+} hereafter, but we note that the apparent charges do not fully correspond to the ideal values. The apparent charge separation of 45% of the ideal value (=1) lies within the normal range of 20–65 % found in charge-ordered manganites and other transition metal oxides.[19–23]

The reduction in structurally observed charge separation is generic for symmetry-broken, charge-ordered transition metal oxides. The origin of this phenomenom remains unclear. However, it is apparent that the transition metal cations are adopting one of two electronic states rather than arbitrary

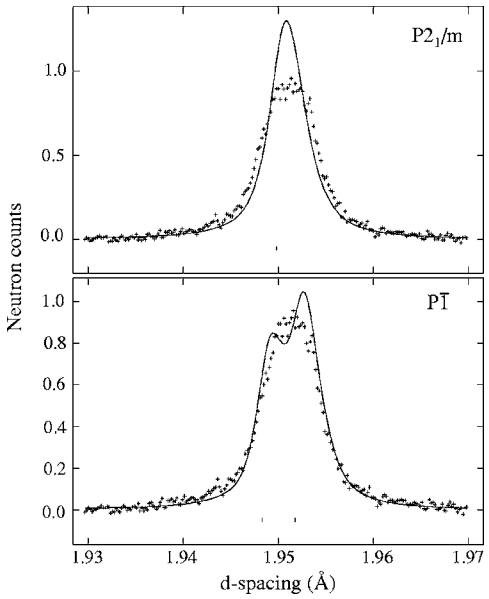

FIG. 3. Excerpts from the Rietveld (whole profile) fits to the time-of-flight powder neutron diffraction data for $YBaMn_2O_6$ at 300 K showing the (220) peak. The monoclinic $P2_1/m$ symmetry model (upper panel) predicts only a single Bragg reflection and gives a poor fit, whereas the triclinic $P\bar{1}$ model (lower panel) that describes the FOO distortions gives partially resolved (220) and $(2\bar{2}0)$ components that fit the peak width correctly.

nonintegral values, which could vary continuously over some range as found in classic charge-density wave materials. This is most strongly evidenced in NaV_2O_5,[21] in which the local structure around eight independent V sites was analyzed. Four of the V sites BVS's cluster around one value (4.2; the V^{4+} state) and the other four cluster around 4.8 (V^{5+}).

TABLE I. Refined atomic parameters for the triclinic $P\bar{1}$ $YBaMn_2O_6$ superstructure at 300 K ($\chi^2=10.44$, $R_{wp}=6.44\%$ for ten atoms, 30 variable coordinates). The labeling of oxygen sites shows the four unique sites in the higher-symmetry $P2_1/m$ structure. Isotropic thermal parameters U_{iso} for the Mn sites, and for the split O1 and O4 sites, were constrained to be equal.

Atom	x	y	z	U_{iso} (Å^2)
Y	0.7546(9)	0.2455(9)	0.5061(8)	0.0271(6)
Ba	0.7557(10)	0.2439(11)	−0.0086(9)	0.0131(8)
Mn1	0.2430(8)	0.2465(14)	0.2579(9)	0.0084(4)
Mn2	0.2518(8)	0.2617(14)	−0.2528(9)	0.0084(4)
O1(a)	0.4828(7)	0.5012(10)	0.2950(6)	0.0284(8)
O1(b)	0.5195(9)	0.0147(10)	0.2529(6)	0.0284(8)
O2	0.2556(8)	0.2776(9)	−0.0047(9)	0.0148(9)
O3	0.1981(8)	0.2026(10)	0.5042(6)	0.0263(9)
O4(a)	0.0222(7)	−0.0348(9)	0.2649(5)	0.0219(8)
O4(b)	−0.0314(8)	0.4881(8)	0.2940(6)	0.0219(8)

TABLE II. Mn-O distances (Å) for the two octahedra in $YBaMn_2O_6$. Values for *trans* pairs of bonds are shown side by side, below the mean value for each octahedron.

	⟨Mn1-O⟩		1.977(8)
O1(a)	1.947(8)	O4(a)	1.971(8)
O1(b)	1.993(9)	O4(b)	2.039(8)
O2	2.005(9)	O3	1.906(8)
	⟨Mn2-O⟩		1.931(8)
O1(a)	1.989(7)	O4(a)	1.963(7)
O1(b)	1.981(9)	O4(b)	1.866(9)
O2	1.889(9)	O3	1.898(8)

Although the MnO_6 octahedra in the monoclinic $P2_1/m$ description of the $YBaMn_2O_6$ structure are irregular, neither one has locally centric distortions of E_g-mode symmetry that would signify orbital ordering. The distortion from monoclinic to triclinic $P\bar{1}$ symmetry breaks the equivalence of the O1(a) and O1(b) sites, and of O4(a) and O4(b) (Table I). The consequence of this is seen in the Mn-O distances (Table II) derived from the freely refined atom coordinates. A further distortion, of E_g symmetry, is observed around Mn^{3+} as the O1(b)-Mn1-O4(b) *trans* pair of distances are longer, by 0.05 and 0.07 Å, than those in the O1(a)-Mn1-O4(a) *trans* pair. The elongated bonds are all approximately parallel to the $[\bar{1}10]$ direction (Fig. 4), corresponding to a ferro-orbital ordering at the Mn^{3+} sites. The Mn^{3+} FOO results in E_g symmetry distortions at the Mn^{4+} sites, as shown in Fig. 1(b), whereas the more common AFOO results in acentric distortions at Mn^{4+} [Fig. 1(a)], as observed, e.g., in $Pr_{0.5}Ca_{0.5}MnO_3$.[9] The octahedral distortions (Table II) in the triclinic $YBaMn_2O_6$ structure are thus a superposition of the mainly acentric distortions that result from Y/Ba cation order, breathing-type centric distortions from Mn^{3+}/Mn^{4+} charge order, and the centric E_g modes that result from ferro-

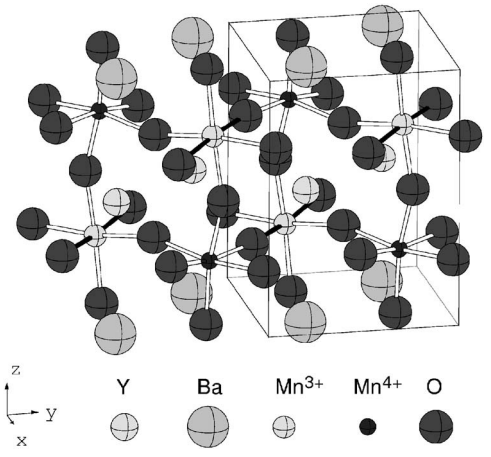

FIG. 4. The 300 K triclinically distorted perovskite structure of $YBaMn_2O_6$ showing order of Y/Ba cations, Mn^{3+}/Mn^{4+} charge states, and Mn^{3+} orbital distortions (elongated Mn-O bonds are shaded black). The ferro-orbital ordering does not double the y-axis periodicity, whereas this is doubled in the antiferro-orbitally ordered analog $TbBaMn_2O_6$.

orbital ordering. FOO has not been reported in other $A\mathrm{MnO_3}$ type manganites, although AFOO is common. This may be in part because FOO states are difficult to detect as they give rise only to (000) (Γ-point) distortions. Our discovery of a subtle triclinic distortion in the 300 K structure of $\mathrm{YBaMn_2O_6}$ is consistent with an electron microscopy study that showed extensive microtwinning.[13] Additional weak $\left(\frac{1}{2}\frac{1}{2}\frac{1}{2}\right)$ superstructure was seen in some images, which may evidence more complex local charge and orbital orderings, but this superstructure is not seen in our neutron data.

The 300 K structures of $\mathrm{YBaMn_2O_6}$ and $\mathrm{TbBaMn_2O_6}$ are both triclinically distorted variants of the parent, charge-ordered $P2_1/m$ arrangement. $\mathrm{YBaMn_2O_6}$ has FOO and no enlarged superstructure, whereas $\mathrm{TbBaMn_2O_6}$ has an additional $\left(0\frac{1}{2}0\right)$ propagation vector, and a partially constrained refinement of the atomic positions showed that AFOO is present.[10] Although the ferrodistortive strain associated with the formation of a FOO state in a high-symmetry parent structure is greater than that required to form an AFOO state,[11] these results show that the two states are of comparable stability in the inherently distorted $R\mathrm{BaMn_2O_6}$ perovskites. The slightly greater disparity in size between R^{3+} and $\mathrm{Ba^{2+}}$ for R=Y compared to R=Tb changes the ground state from AFOO in the latter material to FOO in the former. The comparable stability of the two states is corroborated by a high-temperature neutron diffraction experiment (full results of which will be reported elsewhere). The CO and FOO distortions in $\mathrm{YBaMn_2O_6}$ persist up to a simultaneous charge- and ferro-orbital-ordering transition at $T_{CO}=T_{FOO}=498$ K. However, $\mathrm{TbBaMn_2O_6}$ shows two transitions. The superstructure peaks that characterize the $\left(0\frac{1}{2}0\right)$ AFOO distortion disappear at ~370 K [see Fig. 2(c)] evidencing a transition from AFOO to a FOO structure (like that of $\mathrm{YBaMn_2O_6}$), and the CO and FOO melt at 473 K.

Comparison of these manganites to other CO perovskite oxides shows that high T_{CO}'s are found when the structure is highly distorted from the ideal cubic structure. Nickelate perovskites[24] such as $\mathrm{YNiO_3}$ are distorted through having small A-site cations and have T_{CO} up to 582 K. $(\mathrm{Bi,Sr})\mathrm{MnO_3}$ manganites, which have local off-center distortions due to the bismuth nonbonding electron pair, are charge ordered up to 475 K.[25,26] In $R\mathrm{BaMn_2O_6}$ (R=Tb,Y) phases, internal distortions caused by the size mismatch of R^{3+} and $\mathrm{Ba^{2+}}$ cations lead to T_{CO}'s up to 498 K, accompanied by FOO or AFOO.

In conclusion, we note that the remarkable interplay between the spin, charge, and orbital degrees of freedom in $A\mathrm{MnO_3}$ manganites enables all of the ferro- and antiferro-ordered ground states to be observed by tuning the A-cation composition and ordering. Ferromagnetic (e.g., in $\mathrm{La_{0.7}Sr_{0.3}MnO_3}$) or antiferromagnetic (in $\mathrm{LaMnO_3}$) spin orderings are found; charge orderings can be ferro-checkerboard (striped, in $\mathrm{La_{0.5}Ca_{0.5}MnO_3}$) or antiferro-checkerboard (rocksalt, in $\mathrm{Tb_{0.5}Ba_{0.5}MnO_3}$); and now both ferro-orbital (in $\mathrm{Y_{0.5}Ba_{0.5}MnO_3}$) and antiferro-orbital (in $\mathrm{Tb_{0.5}Ba_{0.5}MnO_3}$) ordered states have been characterized.

ACKNOWLEDGMENTS

We thank EPSRC for the provision of neutron beam time, and Dr. R. Ibberson (ISIS) for his assistance with data collection. A.J.W. acknowledges EPSRC and the Rutherford Appleton Laboratory for support.

[1] *Colossal Magnetoresistance, Charge Ordering and Related Properties of Manganese Oxides*, edited by eds. C. N. R. Rao and B. Raveau (World Scientific, Singapore, 1998); *Colossal Magnetoresistive Oxides*, edited by Y. Tokura (Gordon and Breach Science, New York, 2000).

[2] J. B. Goodenough, Phys. Rev. **100**, 564 (1955).

[3] E. O. Wollan and W. C. Koehler, Phys. Rev. **100**, 545 (1955).

[4] P. G. Radaelli, D. E. Cox, M. Marezio, and S.-W. Cheong, Phys. Rev. B **55**, 3015 (1997).

[5] P. G. Radaelli, D. E. Cox, M. Marezio, S.-W. Cheong, P. E. Schiffer, and A. P. Ramirez, Phys. Rev. Lett. **75**, 4488 (1995).

[6] P. M. Woodward, D. E. Cox, T. Vogt, C. N. R. Rao, and A. K. Cheetham, Chem. Mater. **11**, 3528 (1999).

[7] J. Blasco, J. Garcia, J. M. de Teresa, M. R. Ibarra, J. Perez, P. A. Algarabel, C. Marquina, and C. Ritter, J. Phys.: Condens. Matter **9**, 10321 (1997).

[8] O. Richard, W. Schuddinck, G. Van Tenderloo, F. Millange, M. Hervieu, V. Caigneart, and B. Raveau, Acta Crystallogr., Sect. A: Found. Crystallogr. **55**, 704 (1999).

[9] R. J. Goff and J. P. Attfield, Phys. Rev. B **70**, 140404(R) (2004).

[10] A. J. Williams and J. P. Attfield, Phys. Rev. B **66**, 220405(R) (2002).

[11] D. I. Khomskii and K. I. Kugel, Phys. Rev. B **67**, 134401 (2003).

[12] T. Nakajima, H. Kageyama, and Y. Ueda, J. Phys. Chem. Solids **63**, 913 (2002).

[13] T. Nakajima, H. Kageyama, M. Ichihara, K. Ohoyama, H. Yoshizawa, and Y. Ueda, J. Solid State Chem. **177**, 987 (2004).

[14] J. P. Chapman, J. P. Attfield, M. Molgg, C. M. Friend, and T. P. Beales, Angew. Chem. **35**, 2482 (1996).

[15] F. Millange, E. Suard, V. Caignaert and B. Raveau, Mater. Res. Bull. **34**, 109 (1999).

[16] A. C. Larson and R. B. Von Dreele, Los Alamos National Laboratory Report No. LAUR 86-748, 1994 (unpublished).

[17] This distortion was not resolved in a constant-wavelength neutron diffraction study of $\mathrm{YBaMn_2O_6}$ in Ref. 13. The reported monoclinic $P2$ symmetry model gives a significantly poorer fit to our data (residuals $\chi^2=13.04$, $R_{wp}=7.15\%$ for 14 atoms, 25 variable coordinates).

[18] This estimation of the formal cation charge uses the method and parameters in N. E. Brese and M. O'Keeffe, Acta Crystallogr., Sect. B: Struct. Sci. **47**, 912 (1991).

[19] P. Karen, P. Woodward, J. Linden, T. Vogt, A. Struder, and P. Fischer, Phys. Rev. B **64**, 214405 (2001).

[20] The highest value found for $\mathrm{Mn^{3+}/Mn^{4+}}$ order is 62% in $(\mathrm{Na_{0.25}Mn_{0.75}})\mathrm{MnO_3}$; A. Prodi *et al.*, Nat. Mater. **3**, 48 (2004).

[21] H. Sawa, E. Ninomiya, T. Ohama, H. Nakao, K. Ohwada, Y. Murakami, Y. Fujii, Y. Noda, M. Isobe, and Y. Ueda, J. Phys. Soc. Jpn. **71**, 385 (2002).

[22] J. Rodriguez-Carvajal, G. Rousse, C. Masquelier, and M. Hervieu, Phys. Rev. Lett. **81**, 4660 (1998).
[23] T. Vogt, P. M. Woodward, P. Karen, B. A. Hunter, P. Henning, and A. R. Moodenbaugh, Phys. Rev. Lett. **84**, 2969 (2000).
[24] J. A. Alonso, J. L. Garcia-Munoz, M. T. Fernandez-Diaz, M. A. G. Aranda, M. J. Martinez-Lope, and M. T. Casais, Phys. Rev. Lett. **82**, 3871 (1999).
[25] C. Frontera, J. L. Garcia-Munoz, A. Llobet, M. A. G. Aranda, C. Ritter, M. Respaud, and J. Vanacken, J. Phys.: Condens. Matter **13**, 1071 (2001).
[26] J. L. Garcia-Munoz, C. Frontera, A. Llobet, M. A. G. Aranda, C. Ritter, M. Respaud, and J. Vanacken, Phys. Rev. B **63**, 064415 (2001).